Content

A

5' miR-30: **CTCGAG**AAGGTATATTGCTGTTGACAGTGAGCG

Loop: TAGTGAAGCCACAGATGTA

3' miR-30: TGCCTACTGCCTCG**GAATTC**

The restriction sites are highlighted in bold purple

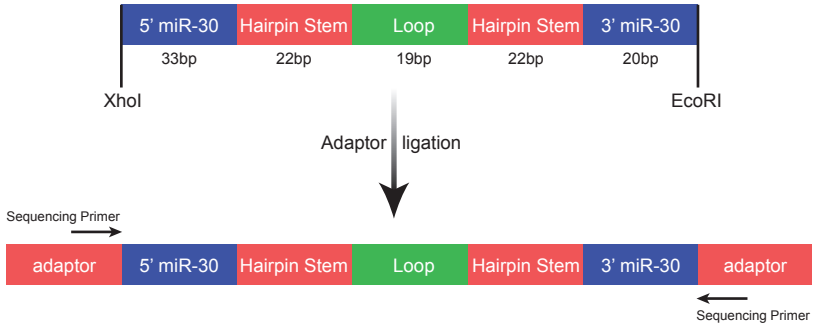

B

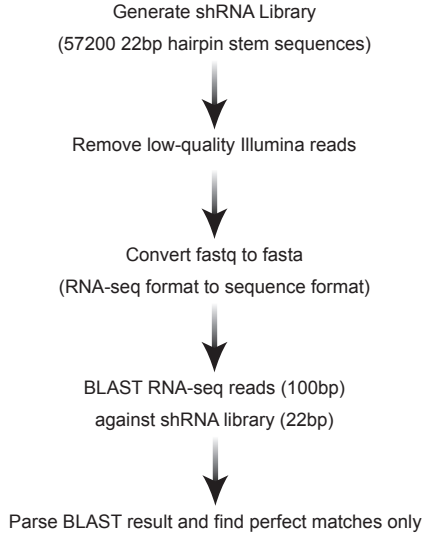

Appendix Figure S1

A Strategy for DNA-seq sample preparation.

B Workflow of sequencing data analysis.

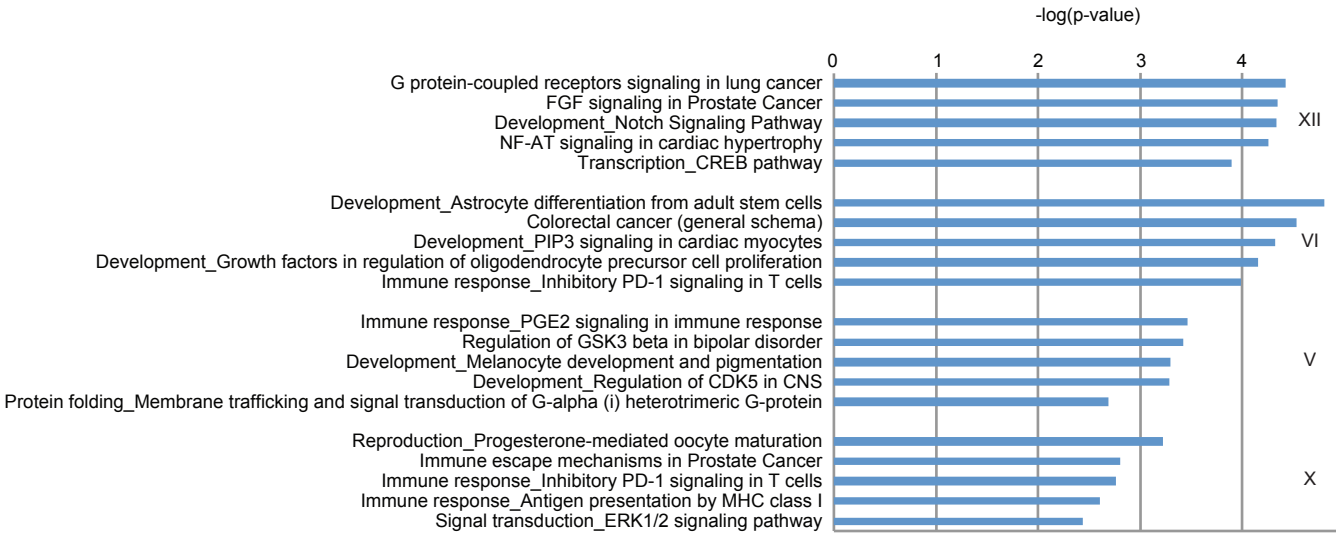

Appendix Figure S2

GO analysis showing the enriched pathways in Group XII, VI, V, and X, which correspond to D6F, D20LS, D20LK, and D20LSK, respectively.

Appendix Figure S3

Validation of the splicing effect and knockdown efficiency of targeted splice-blocking morpholinos targeting Prdm16 (A), Lrsam1 (B), Ap2a1 (C), Hal (D), Mettl22 (E) via RT-PCR and qRT-PCR, with demonstration of morphant phenotype by c-*Myb* in situ at 54 hpf demonstrating decreased HSCs in the dorsal aorta region (F, arrows). Expected product sizes are indicated, with splice-blocking MO-injected embryos demonstrating aberrant splicing via exon-skipping and/or intron retention. Morpholinos targeting the boundary of exon 2 and intron 2 were designated e2i2, while morpholino e1i1 indicated the morpholino targeting the boundary of exon 1 and intron 1. Three primer sets were used to measure the splicing effect. Primer set “a” served as control, while primer sets “b” and “c” were used to examine the splicing alterations. Splice-blocking MO-injected embryos demonstrated aberrant splicing via exon-skipping, intron retention, and/or cryptic-site splicing.

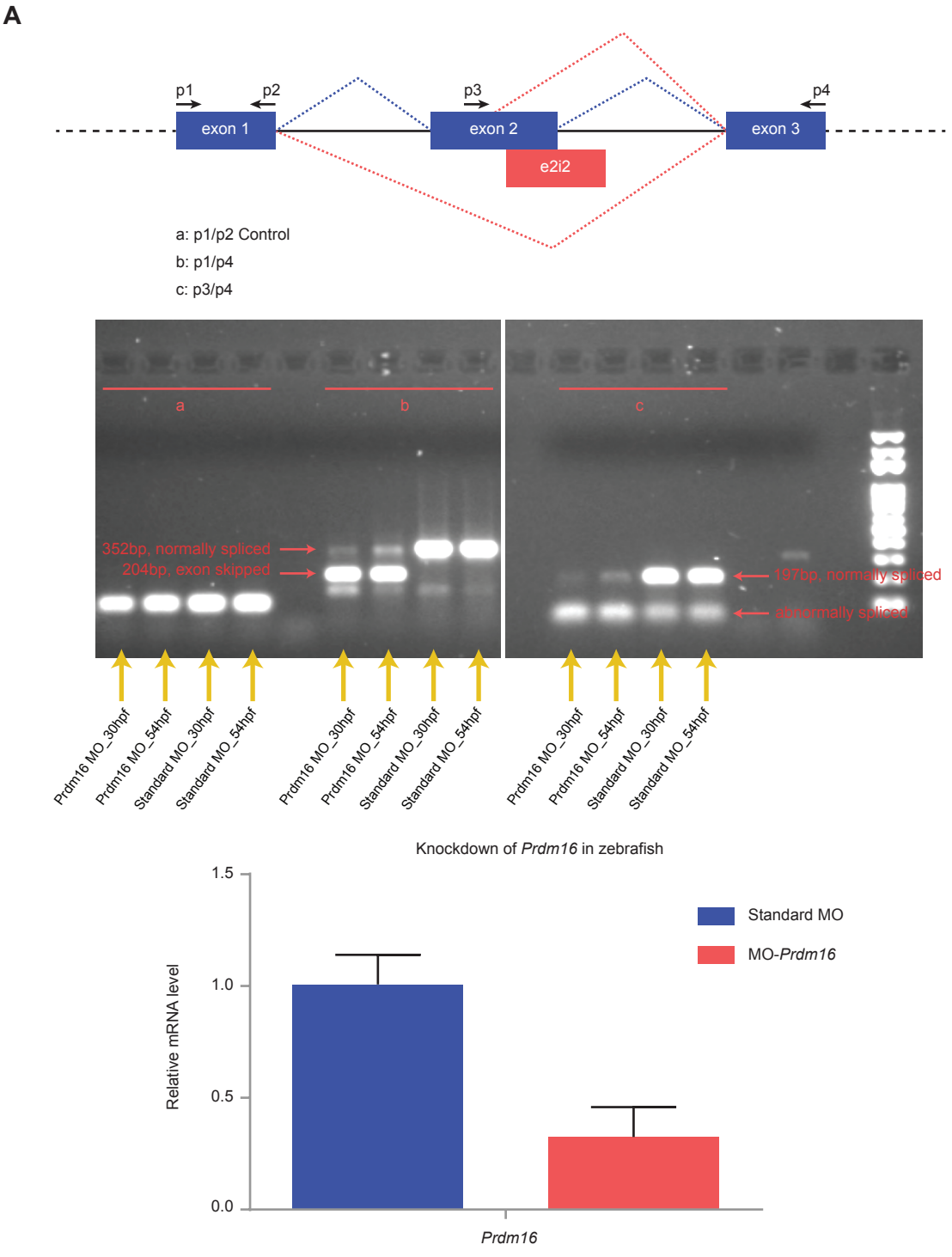

Appendix Figure S3A

RT-PCR showed that e2i2 morpholino targeting Prdm16 caused abnormal splicing of Prdm16 as indicated by primer set b and c. The qRT-PCR was performed using primer set c.

B

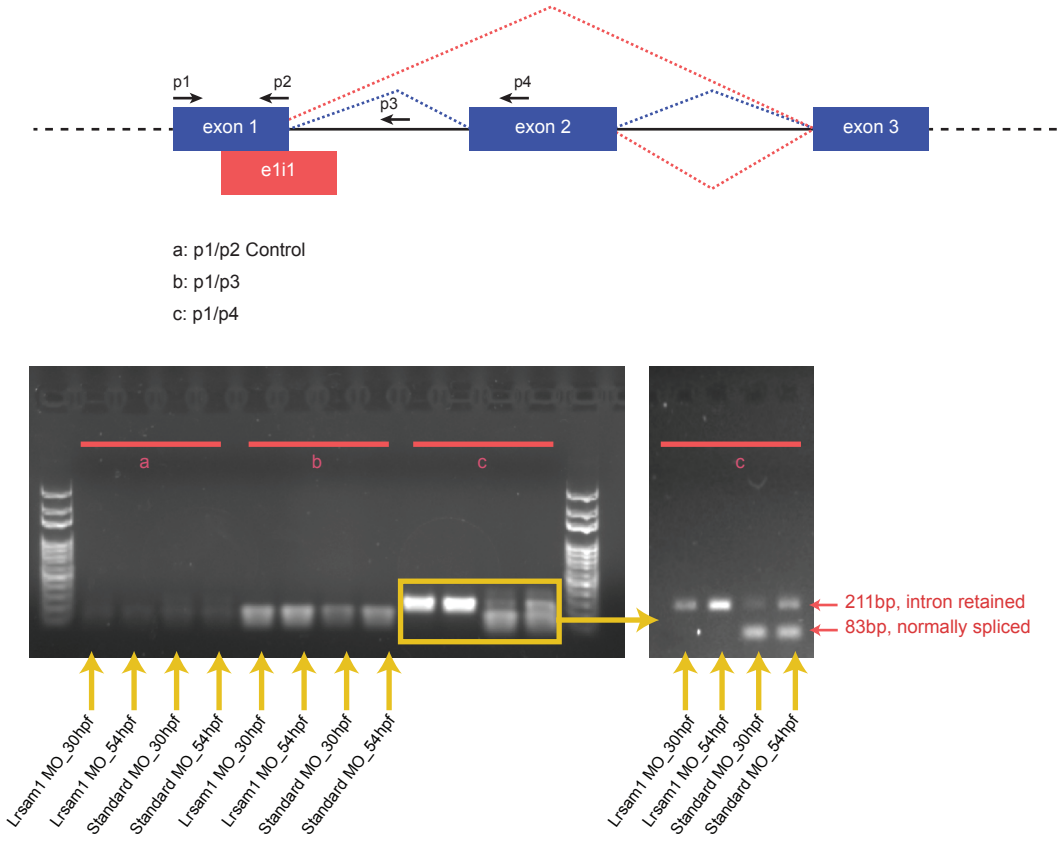

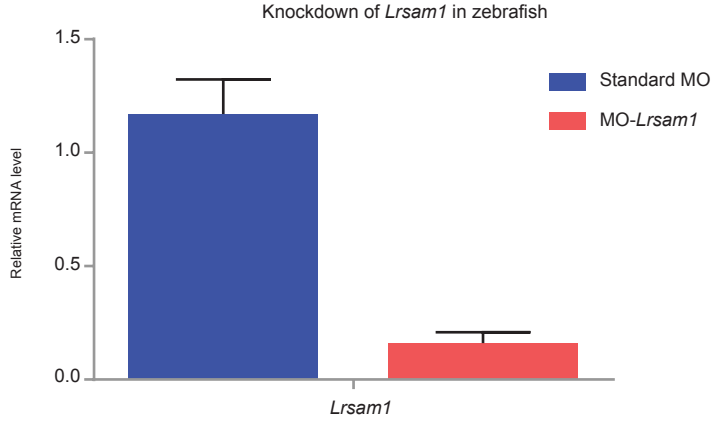

Appendix Figure S3B
Morpholino e1i1 targeting Lrsam1 resulted in intron retention (211bp PCR product amplified with primer set c), which was exclusively present in Lrsam1 MO-injected animals but only a small fraction of controls. Note the absence of detectable correctly spliced product (83 bp) in the MO-injected embryos. Primer set c was used to analyze the knockdown efficiency of Lrsam1 by qRT-PCR. Note that a short cycle time was used for this qRT-PCR experiment in order to preferentially amplify the smaller 83bp product, which was confirmed by post-hoc melting curve analysis.

C

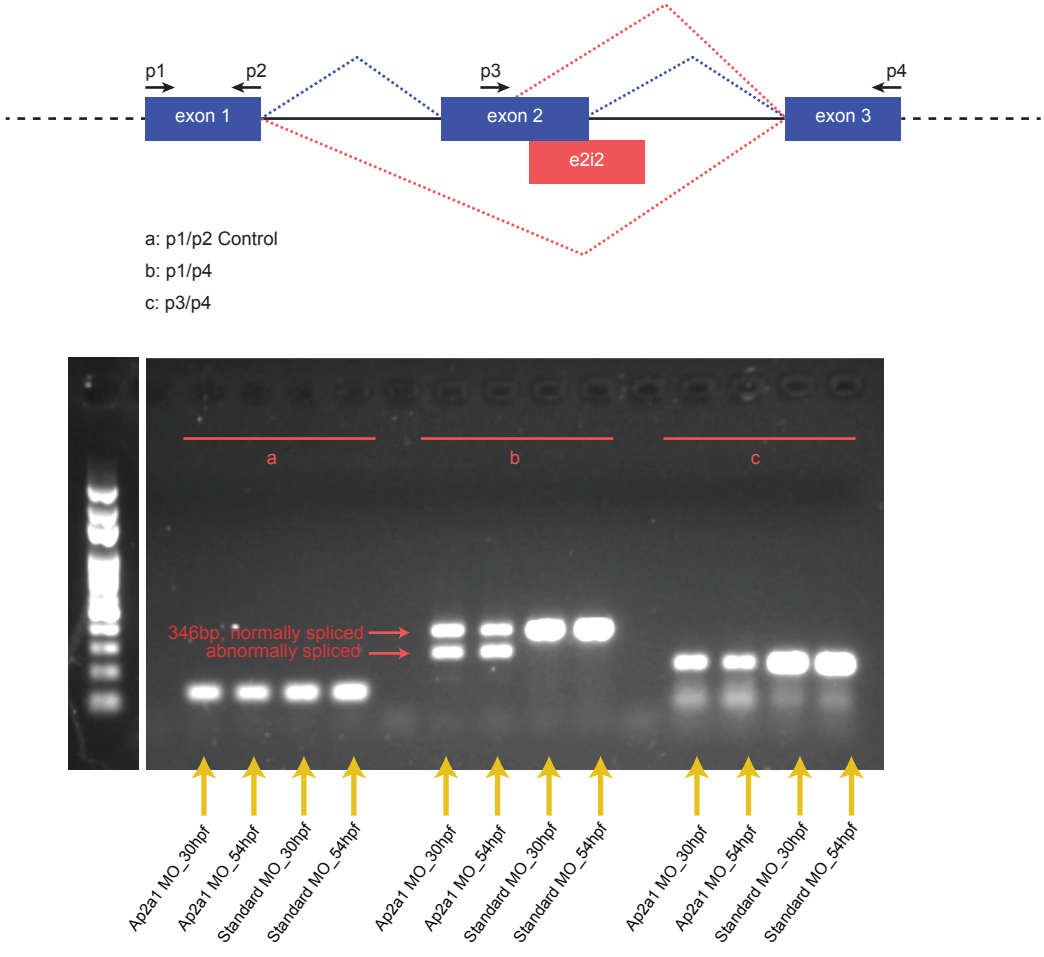

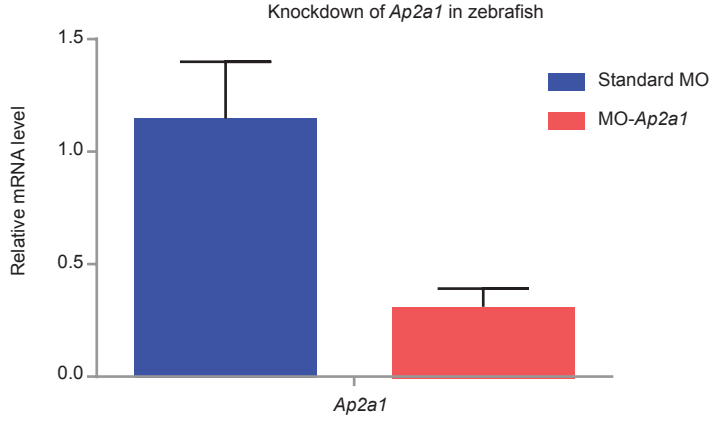

Appendix Figure S3C
Ap2a1 morpholino e2i2 caused abnormal splicing in Ap2a1 mRNA as shown in RT-PCR with primer set b. qRT-PCR was performed using primer set c and the result showed dramatic decrease of mRNA level of Ap2a1.

D

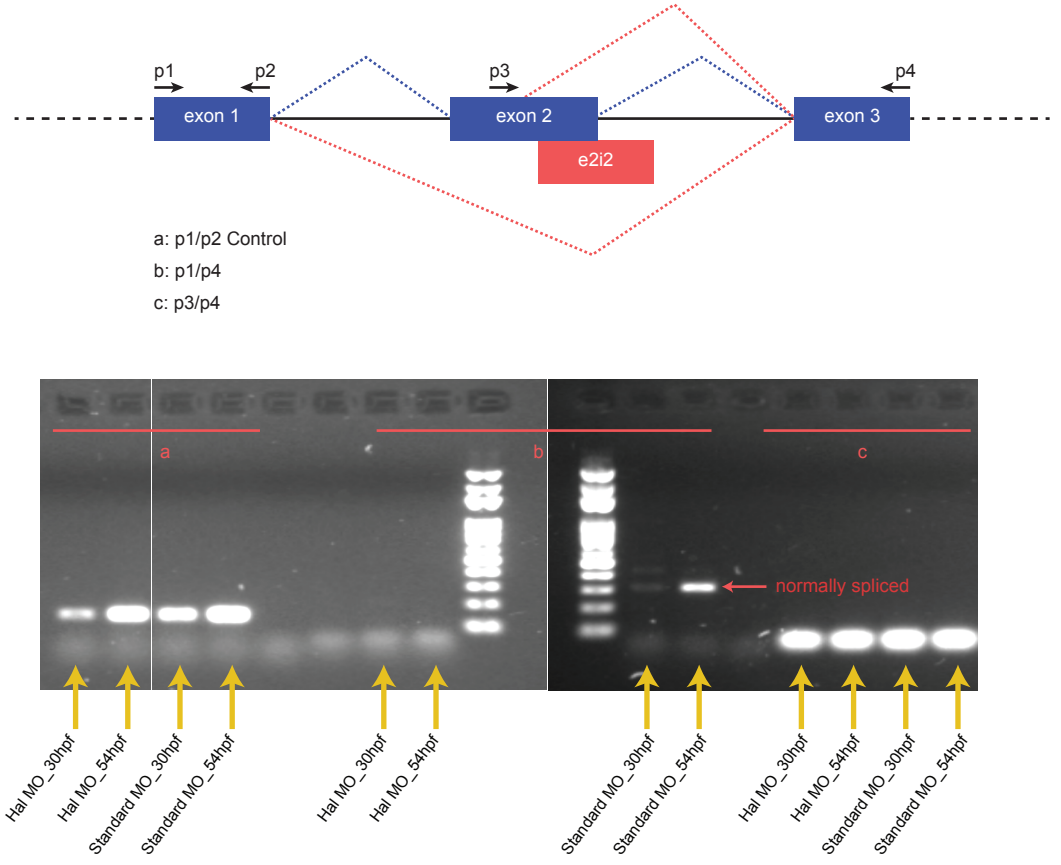

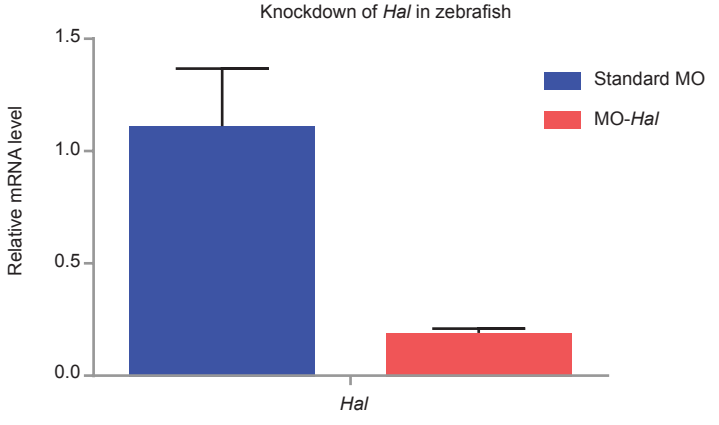

Appendix Figure S3D

RT-PCR analysis showed no band in Hal morpholino injected fish, while expected PCR bands were observed in controls as shown by primer set b. It is likely that the Hal morpholino is causing intron retention (as demonstrated for the Lrsam1 MO in panel B), but in this case we would not expect a PCR product since the second intron of Hal is 2226bp in length. Decreased expression of normal Hal transcript by MO injection was further validated by qRT-PCR using primer set c.

E

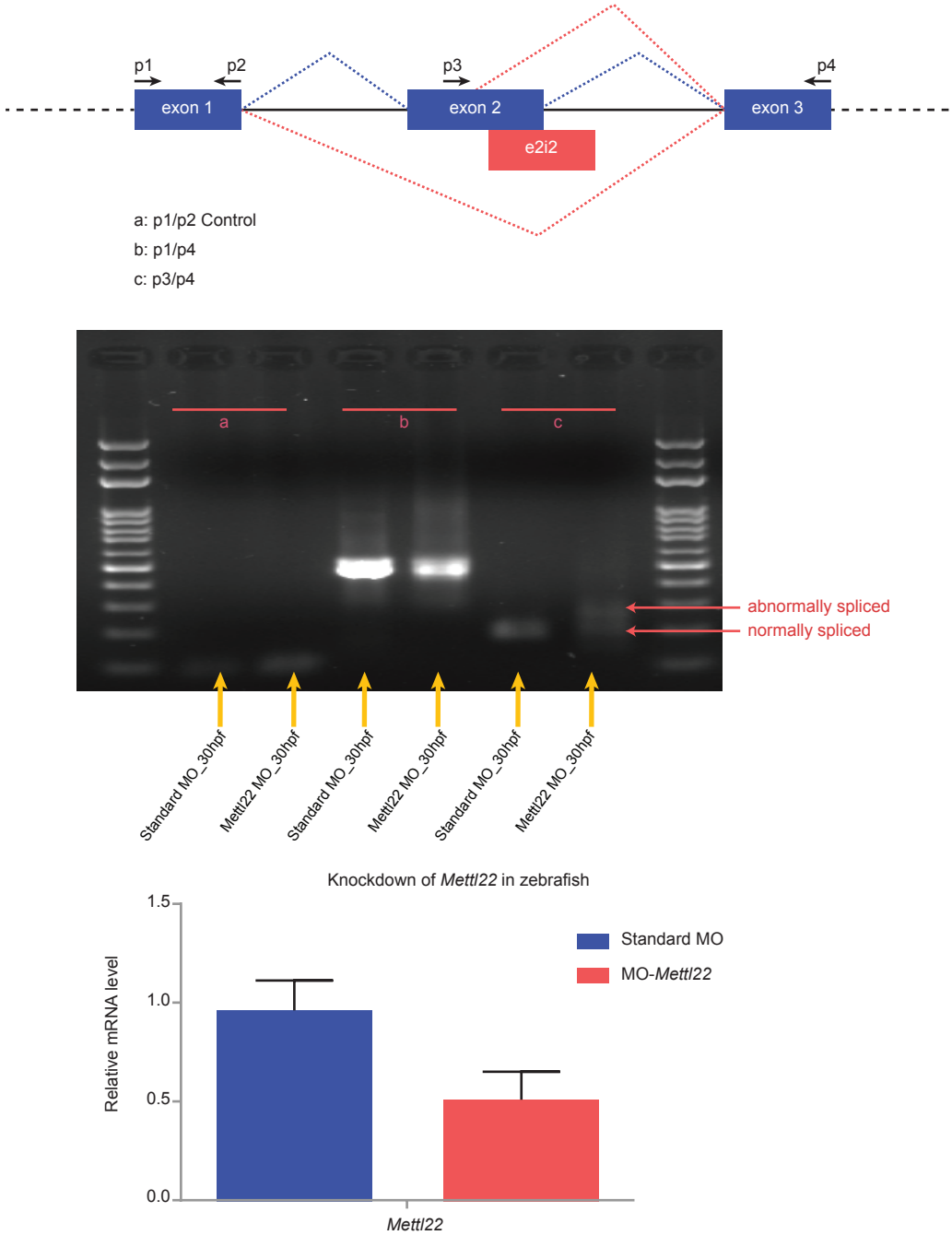

Appendix Figure S3E

RT-PCR analysis showed that morphonilo e2i2 targeting Mettl22 caused abnormal splicing as shown by primer set c. The decrease of normal primer set b PCR product was also observed in Metll22-MO injected fish. Quantification of normal transcript of Mettl22 via qRT-PCR showed strong knockdown effect of morphonilo e2i2 with primer set c.

F

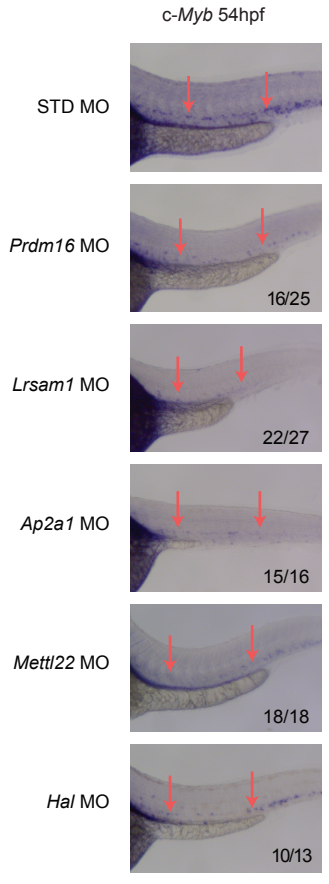

Appendix Figure S3F
Whole-mount in situ hybridization of c-*Myb* expression in zebrafish at 54 hpf showed that MO-mediated knockdown of Lrsam1, Ap2a1, Mettl22, and Hal notably reduced c-*Myb* staining in discrete cells in the ventral region of the dorsal aorta (arrows). Prdm16 knockdown serves as a positive control. Note that nonspecific staining for c-*Myb* was largely unaffected by targeted MO knockdown.